

**SEDIMENT TRANSPORT AND AQUEOUS ALTERATION IN A MARS-ANALOG GLACIAL SYSTEM.**

E. R. Bamber<sup>1</sup>, E.B. Rampe<sup>2</sup>, B. Horgan<sup>3</sup>, R. J. Smith<sup>3</sup>, N. A. Scudder<sup>3</sup>, A. M. Rutledge<sup>3</sup>, <sup>1</sup>Department of Earth Sciences, University of Oxford, Oxford, UK, <sup>2</sup>Astromaterials Research and Exploration Science Division, NASA Johnson Space Centre, Houston, TX, USA, <sup>3</sup>Department of Earth, Atmospheric, and Planetary Sciences, Purdue University, West Lafayette, IN, USA. Emily.Bamber@spc.ox.ac.uk

**Introduction:**

The bulk of the martian crust is basaltic [1, 2] with a wide variety of subsequently derived aqueous alteration phases [3-5]. Study of analogue terrains is vital to better understand the weathering of such mafic bedrock at a range of surface temperatures. Moreover, climatic models have suggested that the early martian climate was not warm and wet, but cold and icy [6], with some of the apparent fluvial and lacustrine features attributable to transient melting of ice sheets as opposed to persistent surface water [e.g. 6, 7].

This study examines sediment samples from Collier glacial valley, Three Sisters, Oregon (OR), with the aim of better characterizing erosion, transport, and *in situ* aqueous alteration in a glaciated Mars-analogue terrain.

**Methods:**

Collier glacier drains dacite, andesite, and basaltic andesite units [8, 9; Figure 1]. Basaltic andesite units show evidence of hydrothermal alteration.

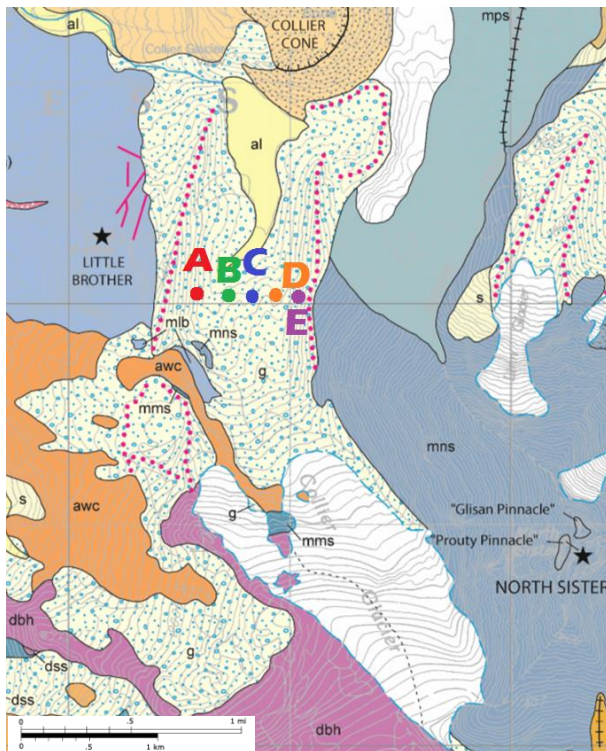


**Figure 1:** Geological map of the area surrounding Collier glacier, adapted from [9]. mlb=mafic Little Brother (basaltic andesite); mns=mafic North Sister (basaltic andesite); mms=mafic Middle Sister (basaltic andesite); awc=andesite of west Collier; dbh=dacite of Black Hump. The locations of samples A-E along an east-west transect are indicated.

Samples were sieved to eight particle size fractions corresponding to divisions in the Wentworth classification and the %wt for each size-component was measured. Samples were spiked with 20 wt% corundum as an internal standard for X-ray diffraction (XRD). XRD patterns were measured from 2-80 °2θ at 100 seconds per step with a 0.0167° step size, in a Panalytical X'Pert Pro instrument with a Co-Kα source. Mineral abundances were determined using the Panalytical High Score Plus software (HSP) which, combined with measurement uncertainty, has a detection limit of 2-3%wt. Rietveld refinement was conducted using the Jade software package, for a transect of moraine samples [Figure 1]. Jade has a detection limit of ~0.5%wt. Six field samples were selected for study in the JEOL 7600F Scanning Electron Microscope (SEM) at Johnson Space Centre, Houston. Secondary electron images and EDS data were obtained at 15kV and 800pA.

**Results:**

The glacial sediments are dominated by the minerals plagioclase feldspar and pyroxene. Upstream and westwards, low-Ca dominates over high-Ca pyroxene. Downstream, pyroxene compositions vary. X-ray amorphous phases were also detected at up to 27%wt. All other phases detected did not exceed 10%wt.

Quartz appears absent from the up-valley, eastern sediments and displays a tendency to be concentrated in the coarser particle size fractions upstream and finer fractions on the banks of the proglacial lake. Magnetite also fines downstream like quartz. Hematite, a less abundant oxide, is associated with coarser grain sizes in the uppermost glacial toe-region and central-eastern side of the valley, close to hydrothermally altered ash units [8] and consistent with remote sensing observations [10]. Ilmenite is detected by Jade and SEM but not HSP, thus its distribution is not yet characterized. Zeolites were not detected using HSP nor SEM, but analysis using Jade identified chabazite in samples B and D on either side of the valley transect.

Potassium feldspar was not detected by HSP, but a K-bearing phase was detected by SEM in samples A and D. Jade suggested up to 5 %wt orthoclase in sample C in the cross-valley transect, but no others [Figure 2]. The X-ray-amorphous content, evident from the broad hump centered around 3.8Å, is quantified using Jade for the east-west valley transect and varies between 0-30%wt [Figure 2]. The composition of such poorly crystalline phases cannot be derived from XRD, but the potential candidates are primary volcanic glass and secondary alteration phases.

Detailed investigation of the trends across the east-west transect revealed that sample mineralogy varies significantly [Figure 2]. Sample C towards the east is notably distinct with potassium feldspar and trace amounts of actinolite within the modelled mineralogy. Zeolite was found in samples B and D. Sample E contains the greatest amorphous content.

#### Discussion:

The varying abundances of certain mineral phases upstream indicates the extent of contribution from the more evolved volcanic rocks (andesite awc and dacite dbh). Increasing low-Ca pyroxene and quartz content eastwards downstream signifies homogenization. More detailed textural and compositional analyses of primary phases could expose trends not noted here.

The concentration of quartz and oxides in finer fractions downstream is consistent with physical weathering during glacial transport of bedrock. However, due to the low %wt of such phases, close to the detection limit of HSP, patterns require confirmation by Jade.

Crystalline alteration phases (zeolites and hematite) are detected at low %wt in samples and are most likely derived from altered units on North Sister and Little Brother [Figure 1; 8]. The absence of any significant amounts of crystalline phases formed *in situ* indicates that glacial environments lead to minimal chemical alteration. However, amorphous alteration phases may be present since the amorphous hump in XRD patterns is not entirely consistent with just volcanic glass [10, 11]. Transmission electron microscopy of sediment samples [12] has identified several of these phases including nanophase iron oxides and “proto-clays”. Observations of similar amorphous materials on Mars [3, 4, 13-16] may be evidence of the Red Planet’s ancient glaciated surface.

Across the east-west transect, mineralogical variations indicate bedrock source units for each sample [Figure 2]. For example, the distinct mineralogy of sample C replicates that of the unit awc [Figure 1]. However, sample E has a much higher amorphous content than its adjacent unit mns, potentially due to the *in situ* formation of amorphous alteration phases.

Overall, the olivine content is less than that of the mafic source units, indicating increased dissolution relative to other primary phases.

#### Conclusions:

The main downstream trends are the increased mixing of phases and confinement of rarer minerals to fine-grained fractions. Cross-valley mineralogical variations are clearly related to the bedrock source region, except for in olivine and amorphous content which may comprise the main weathering signature of mafic glacial terrains. The near absence of crystalline alteration phases confirms there is minimal chemical alteration.

In comparison to Mars, the wide variety of secondary phases [5] detected by the *Curiosity* at Gale Crater [17], could not be produced in a glacial terrain similar to the Three Sisters volcanic complex. On the other hand, the amorphous content at Gale [13-16] is comparable to that of Collier glacial valley and probably not produced by a warm, wet climate. Some work has addressed the nature of the amorphous phases within Collier [11, 12, 18], but more is needed to further characterize the unique weak alteration signatures produced in a mafic glacial terrain.

#### Acknowledgements:

We are grateful to Dr. Eve Berger for helpful comments related to SEM work. We thank LPI, USRA, and colleagues at NASA JSC for supporting Emily Bamber as a summer intern to undertake this research.

**References:** [1] A. D. Rogers and P. R. Christensen (2007) *JGR*, 112: E01003 [2] H. Y. Mcsween et al. (2009) *Science*, 324: 736-739 [3] B. Horgan and J. Bell (2012) *Geology*, 40: 391-394 [4] E. B. Rampe et al. (2012) *Geology*, 40: 995-998 [5] B. L. Ehlmann and C.S. Edwards (2014) *Annu. Rev. Earth Planet. Sci.*, 42:291–315 [6] R. Wordsworth et al. (2013) *Icarus*, 222: 1-19 [7] J. W. Head and D. R. Marchant (2014) *Antarctic Science*, 26(6): 774-800 [8] M. E. Schmidt and A. L. Grunder (2009) *GSA bulletin*, 121: 643-662 [9] W. Hildreth et al. (2012) *USGS, Scientific Investigations Map 3186* [10] N. A. Scudder et al. (2017) *LPSC XLVIII #2625* [11] R. J. Smith et al. (2017) *LPSC XLVIII, #2465* [12] E. B. Rampe et al. (2017) *GSA Annual Meeting* [13] D. L. Bish et al. (2013) *Science*, 341(6153): 1238932 [14] D. F. Blake et al. (2013) *Science*, 341(6153): 1239505 [15] D.T. Vaniman et al (2014) *Science*, 343(6169):1243480 [16] R. V. Morris et al. (2015) *LPSC XLVI #2434* [17] E. B. Rampe et al. (2016) *LPSC XLVII #2543* [18] E. B. Rampe et al (2017) *AGU P33C-2892*.

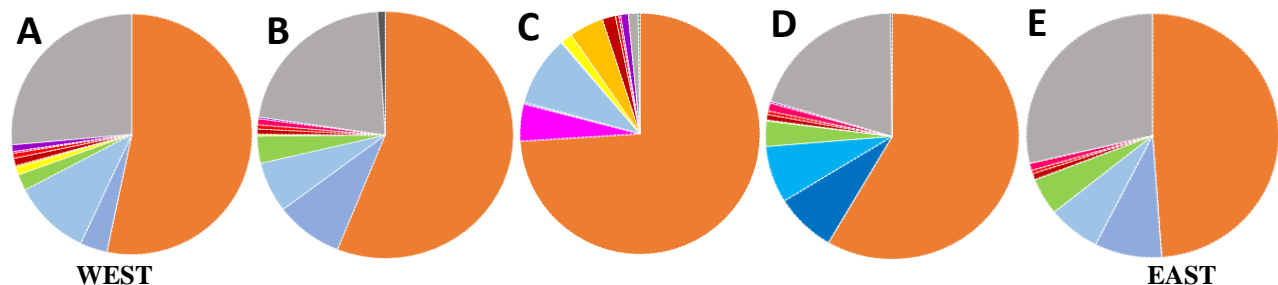


**Figure 2:** Pie charts indicating the weighted average abundance of mineral phases in samples A-E across the central valley transect, as modeled by JADE and weighted by %wt in each particle size fraction. **KEY:** orange = plagioclase (andesine, labradorite, anorthite, albite), pink = Kfs, dark blue = High-Ca px, light blue = low-Ca px, green = olivine, reds = oxides (hematite, magnetite), purple = fluorapatite, light grey = amorphous, dark grey = zeolite, dark green = actinolite